Mon. Not. R. Astron. Soc. **000**, 1–?? (2016) Printed 20 September 2016 (MN LATEX style file v2.2)

New open cluster Cepheids in the VVV survey tightly constrain near-infrared period–luminosity relations

Xiaodian Chen[1,2], Richard de Grijs[1,3] and Licai Deng[2]
[1] *Kavli Institute for Astronomy & Astrophysics and Department of Astronomy, Peking University, Yi He Yuan Lu 5, Hai Dian District, Beijing 100871, China*
[2] *Key Laboratory for Optical Astronomy, National Astronomical Observatories, Chinese Academy of Sciences, 20A Datun Road, Chaoyang District, Beijing 100012, China*
[3] *International Space Science Institute–Beijing, 1 Nanertiao, Zhongguancun, Hai Dian District, Beijing 100190, China*

arXiv:1609.05440v1 [astro-ph.GA] 18 Sep 2016

xxx

ABSTRACT
Classical Cepheids are among the most useful Galactic and nearby extragalactic distance tracers because of their well-defined period–luminosity relations (PLRs). Open cluster (OC) Cepheids are important objects to independently calibrate these PLRs. Based on Data Release 1 of the *VISTA* Variables in the Vía Láctea survey, we have discovered four new, faint and heavily reddened OC Cepheids, including the longest-period OC Cepheid known, ASAS J180342−2211.0 in Teutsch 14a. The other OC–Cepheid pairs include NGC 6334 and V0470 Sco, Majaess 170 and ASAS J160125−5150.3, and Teutsch 77 and BB Cen. ASAS J180342−2211.0, with a period of $\log P = 1.623$ [days] is important to constrain the slope of the PLR. The currently most complete $JHK_{\rm s}$ Galactic Cepheid PLRs are obtained based on a significantly increased sample of 31 OC Cepheids, with associated uncertainties that are improved by 40 per cent compared with previous determinations (in the J band). The NIR PLRs are in good agreement with previous PLRs determined based on other methods.

Key words: methods: data analysis — stars: variables: Cepheids — open clusters and associations: general — stars: distances

1 INTRODUCTION

Classical Cepheids are among the most useful Galactic and nearby extragalactic distance tracers because of their well-established period–luminosity relations (PLRs; also known as the 'Leavitt law': Leavitt & Pickering 1912). Cepheids are commonly used to anchor extragalactic distances, constrain the Hubble constant and study Galactic structure. They also relate directly to secondary distance tracers, such as Type Ia supernovae, whose luminosities are calibrated using Cepheids in their host galaxies (Riess et al. 2011). The Carnegie Hubble Program (Freedman et al. 2011) aims at determining an accurate Hubble constant based on the Cepheid distance scale, Matsunaga et al. (2011, 2015), Feast et al. (2014) and Dékány et al. (2015) have studied the Milky Way's structure in the Galactic bulge based on Cepheids, while Majaess et al. (2009) and Dambis et al. (2015) mapped the Galactic spiral arms using distances to classical Cepheids.

Cepheid PLRs are not only important for measuring distances but also to constrain the pulsation physics and the evolution of Cepheids. However, independent Cepheid distances must be obtained, which can be achieved using (i) trigonometric parallaxes (Feast and Catchpole 1997; Benedict et al. 2007), (ii) Baade–Wesselink-type methods/surface-brightness techniques (Gieren et al. 1997; Storm et al. 2011) and (iii) main-sequence or isochrone fitting based on open cluster (OC) photometry (An et al. 2007; Turner 2010; Anderson et al. 2013; Chen et al. 2015). The OC parameters derived based on the latter method can be used as independent constraints on the distances, ages and reddening values of Cepheids in these clusters. This method can also be used to study Cepheids in heavily reddened environments.

The key to establishing the PLR using OC Cepheids is to select high-confidence cluster Cepheids. An et al. (2007) obtained $BVI_{\rm c}JHK_{\rm s}$ PLRs based on seven Galactic OCs hosting Cepheids, while Anderson et al. (2013) found five OC Cepheids using an eight-dimensional selection approach and obtained a V-band PLR for 18 OC Cepheids. Chen et al. (2015) found six new OC Cepheids based on near-infrared (NIR) data and derived a J-band PLR for 19 OC Cepheids. As more accurate data are becoming available, the number of OC Cepheids is increasing, whereas the confidence of OC membership is improving simultaneously. Majaess et al. (2011) provided new evidence to support the likely membership of the Cepheid TW Nor of the OC Lyngå 6. Turner et al. (2012) discovered that SU Cas

© 2016 RAS

is a probable member of the OC Alessi 95; Majaess et al. (2012) conducted a detailed distance analysis of this latter OC and its member Cepheids based on new X-ray and $JHK_{\rm s}$ data. Majaess et al. (2013) assessed the links between three Cepheids and NGC 6067 based on data from the *VISTA* Variables in the Vía Láctea (VVV) survey. However, the number of OC Cepheids that can presently be used to establish OC–Cepheid PLRs is still small, of order 20. One limitation to further progress is that approximately half of the OCs in the DAML02 catalogue (Dias et al. 2002) are poorly studied. Another limitation is a lack of availability of mean Cepheid intensities in multiple passbands; indeed, for many Cepheids we only have access to their V-band light curves.

In this paper, we use VVV Data Release 1 (DR1) (Minniti et al. 2010; Saito et al. 2012) to study faint OCs in the Galactic bulge and the Galactic midplane. We improve the quality of their age, reddening and distance determinations. We also convert single-epoch NIR photometry to mean intensities based on application of light-curve templates. We have collected the current largest sample of 31 high-confidence OC Cepheids based on NIR photometry, thus enabling us to obtain the most accurate $JHK_{\rm s}$ PLRs for Galactic OC Cepheids to date. In fact, in this paper we derive the first statistically meaningful OC–Cepheid H- and $K_{\rm s}$-band PLRs; our updated J-band PLR represents a significant improvement with respect to our earlier derivation (Chen et al. 2015). In section 2 we present the data, the method used and our OC–Cepheid catalogue. Section 3 discusses the OC membership characteristics of our four newly found Cepheids. In Section 4 we discuss the Cepheid $JHK_{\rm s}$ PLRs, while Section 5 summarizes and concludes this paper.

2 METHOD

NIR $JHK_{\rm s}$ photometry is suitable for studies of young OCs, not only because of the small or even negligible effects expected owing to differential extinction, but also in the context of detecting heavily obscured main-sequence stars (Majaess et al. 2012). Using the Two Micron All-Sky Survey (2MASS) Point Source Catalog (Cutri et al. 2003), thousands of OC parameters can be determined easily using main-sequence fitting. Complete samples can reach distances of order 1.8 kpc (Kharchenko et al. 2013). With the availability of NIR surveys fainter than 2MASS, such as the UKIRT Infrared Deep Sky Survey (UKIDSS) DR6 Galactic Plane Survey (Lucas et al. 2008) and VVV DR1, even more distant, heavily reddened OC properties can be determined. The VVV survey is a $ZYJHK_{\rm s}$ photometric survey focussed on the Galactic Centre and a few fields along the Galactic plane. It reaches four magnitudes fainter than 2MASS. Combining 2MASS $JHK_{\rm s}$ data and VVV data, the available NIR catalogues cover a range of more than 10 magnitudes, thus allowing us to study Galactic stellar populations from bright Cepheids to faint main-sequence dwarf stars.

Cepheids are young stars with ages near $\log(t\ {\rm yr}^{-1}) = 8.0$, so they can be present in young OCs. To find OC Cepheids, we rely on properties such as their spatial positions, distances and proper motions, as well as their radial velocities, ages and metallicities (Anderson et al. 2013; Chen et al. 2015). Usually, the positions and distances are easily obtained, while proper-motion and radial-velocity data are only available for smaller numbers of specific OCs. To define our OC master sample, we included not only the 2167 OCs in the January 2016 version of the DAML02 catalogue, but also some other new OCs recently found by Borissova et al. (2011, 2014), Chené et al. (2012), Schmeja et al. (2014) and Scholz et al. (2015). In addition, we collected all Cepheids in the All-Sky Automated Survey (ASAS) Catalogue of Variable Stars (Pojmanski et al. 2002), the General Catalogue of Variable Stars (GCVS) and Tammann et al. (2003). Positional cross-matching within 1 degree (projected) separation in the VVV field yielded 203 potential OC–Cepheid pairs. In our next selection step we excluded Cepheids that are located more than three times their host OC's apparent radius from the cluster centre, leaving 22 OCs for further analysis.

To obtain stellar samples of genuine OC members, we next proceeded with proper-motion analysis. Proper-motion data were obtained from the the Fourth US Naval Observatory CCD Astrograph Catalog (UCAC4; Zacharias et al. 2013). Stars with proper-motion errors in excess of 20 mas ${\rm yr}^{-1}$ were excluded from our initial samples. Subsequently, we calculated the average and standard deviation for all stars in the distribution so as to exclude high-proper-motion stars, adopting a 1σ selection cut. This process was repeated twice to obtain reliable proper motions for each cluster. All stars located within the 1σ proper-motion distribution were adopted as cluster members, while for some OCs with fewer than 100 stars within the 1σ distribution, we selected all stars inside the 2σ distribution instead. We then selected Cepheids located within the 1σ proper-motion distribution of their host clusters for further analysis: see Fig. 1. To select genuine cluster members, we plotted the $(J, J-H)$ colour–magnitude diagrams (CMDs), combining 2MASS and VVV data. VVV $JHK_{\rm s}$ magnitudes were converted to the 2MASS $JHK_{\rm s}$ system following the prescriptions recommended by the Cambridge Astronomy Survey Unit[1].

For clusters exhibiting obvious main sequences, distances, reddening values and ages can be determined by fitting the cluster sequences with Padova isochrones (Girardi et al. 2000; Bressan et al. 2012). Since OCs generally belong to a relatively young Milky Way population, their metallicities are comparably high, on the order of the solar value. In addition, metallicity-dependent variations in the derived cluster parameters, including the ages and distances, are small (e.g., Kharchenko et al. 2013). Hence, we adopted solar metallicity. The scatter in the cluster sequences is mainly caused by differential reddening and the consequently faint stellar luminosities. We applied our isochrone fitting in an automated fashion to determine the smallest residuals pertaining to the parameter space defined by the cluster ages, reddening values and distance moduli.

For a given isochrone defined by a specific age, reddening and distance modulus, our fitting procedure consisted of four steps. First, we linearly resampled (interpolated) the theoretical isochrone such that the intervals between two adjacent points were about 0.01 mag. Second, we selected the nearest isochrone point to every observed data point and

[1] http://casu.ast.cam.ac.uk/surveys-projects/vista/technical/photometricproperties

determined the distance between each pair of points thus selected. Based on the mean distance and standard deviation, obvious field stars beyond the distribution's 1σ range were excluded. Third, we calculated the mean distance and standard deviation for this initial, cleaned data set. For bright stars, $J < 13.5$ mag, we adopted stars located within the 2σ range as cluster members; for fainter stars, the selection criterion was established independently for every 0.1 mag bin between $J = 13.5$ mag and $J = 19.0$ mag. The standard deviation increases from bright to faint magnitudes. Stars found within the 1σ range in each bin were selected as high-probability OC members. These cluster members are shown in the rightmost panel of Fig. 2. Finally, we calculated the uncertainty in the colour excess, the error in the apparent distance modulus and the overall uncertainty.

Next, we allowed the age (0.1 dex age resolution), reddening (0.01 mag resolution) and distance modulus (0.1 mag resolution) to vary freely in order to find the best fit, i.e., the result defined by the smallest overall error. Figure 2 shows, from left to right and for all four newly found OCs hosting Cepheids, the original CMDs, the control-field CMDs, the cleaned CMDs and the CMDs resulting from our automated fitting. The original CMDs are composed of stars located in the cluster regions and based on 2MASS and VVV data. The control fields are located at least twice the cluster radius from the cluster centre, and the size of the control field is the same as that of the cluster field. Since the VVV fields are very well populated, the control fields could be used to statistically correct for field stars. The cleaned CMDs show the candidate cluster members, resulting from having statistically subtracted the control fields from the cluster fields. They exhibit obvious cluster sequences from the saturation magnitude ($J \sim 12.5$ mag) to $J \sim 17.0$ mag. These sequences are comparable to the sequences resulting from our automated fits (see the rightmost panels in Fig. 2). This confirms that the cluster sequences selected by our automated fits are statistically reliable. We did not fit the field-star-subtracted sequence directly, because the reliable range of object magnitudes is small, and so is the number of sources in the subtracted sequence. Since the VVV survey images were taken with very short exposure times, it is more appropriate (and more statistically meaningful) to perform statistical analyses of large samples instead of analyses based on a smaller number of specific, extracted sources. The basic physical OC parameters thus obtained are included in Table 1. They form the basis for our OC–Cepheid selection. Upon application of all selection criteria, four high-confidence OC–Cepheid pairs remain: see Fig. 2, where we show the approximate locations of the clusters' instability strips. OC Cepheids must be located inside the instability strip of their host cluster.

3 RESULTS: INDIVIDUAL OPEN CLUSTER–CEPHEID MATCHES

The four newly found OC Cepheids are more distant long-period Cepheids, hidden behind heavier extinction, than the OC Cepheids found previously. Their inclusion has the potential to improve the importance of the NIR PLRs' calibrations based on the OC-matching method. In addition,

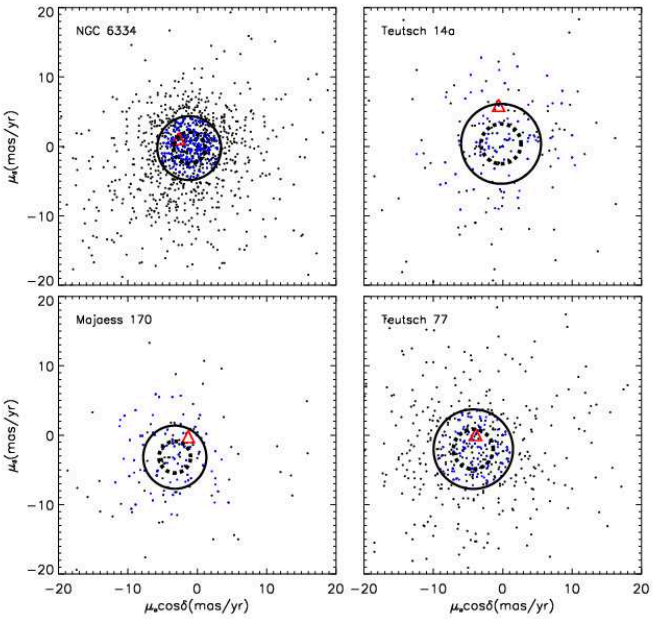

Figure 1. Proper-motion selection of our four target OCs. Solid and dotted circles show, respectively, the 1σ and 0.5σ radii of the clusters' proper motions. Black dots: stars with uncertainties smaller than our error cut of 15 mas yr^{-1} (the typical 1σ uncertainty in the proper-motion catalogue is 4–5 mas yr^{-1}). Blue dots: cluster members located inside the 1σ (well-populated OCs) or 2σ radii (sparsely populated OCs). Red triangles: Cepheid proper motions.

long-period Cepheids (few of which are available to date) are important to accurately determine the slope of the PLRs.

NGC 6334 is a heavily reddened star-forming region. The DAML02 Galactic OC catalogue treats it as an OC with a diameter of 31 arcmin. The VVV NIR data exhibit an obvious OC main sequence (see Fig. 2). Russeil et al. (2012) obtained a distance $d = 1.72 \pm 0.26$ kpc and an extinction of $A_V = 4.52 \pm 0.68$ mag using 11 OB stars. Our isochrone fits yield a distance, colour excess and age of $\mu_0 = 11.16 \pm 0.25$ mag ($d = 1.7 \pm 0.2$ kpc), $E(J-H) = 0.28 \pm 0.02$ mag and $\log(t \text{ yr}^{-1}) = 7.7 \pm 0.3$, respectively. A distance modulus of $\mu_0 = 11.17 \pm 0.38$ mag is determined from the V-band PLR if we adopt the V0470 Sco mean magnitude of $m_V = 11.0$ mag and $A_V = 4.52$ mag. The Cepheid V0470 Sco – $\log P = 1.211$ [days] – is located at roughly 70 arcmin from the centre of NGC 6334, which is well beyond the catalogued size of this cluster. However, a *Herschel* image (Russeil et al. 2013) shows that the cluster's structure extends to a radius of approximately 2 degrees. The radial velocity of V0470 Sco is -3.4 ± 0.5 km s^{-1} (Pejcha & Kochanek 2012), which is comparable to both the HII region's velocity (Anderson et al. 2011) and the mean velocity of the NGC 6334 complex (Russeil et al. 2013). The proper motion of V0470 Sco, $(\mu_{\alpha,\text{Cep}}, \mu_{\delta,\text{Cep}}) = (-2.7 \pm 1.0, 1.1 \pm 2.0)$ mas yr^{-1}, is also in the same range as that of NGC 6334, $(\mu_{\alpha,\text{cl}}, \mu_{\delta,\text{cl}}) = (-1.2 \pm 3.1, -0.2 \pm 3.4)$ mas yr^{-1}. Since Cepheids obey PLR and mass–luminosity relations, the long period of V0470 Sco implies and intrinsically high luminosity, high mass and young age. Bono et al. (2005) provided a straightforward means to calculate Cepheid ages based on theoretical pulsation modelling; they obtained the period–age relation

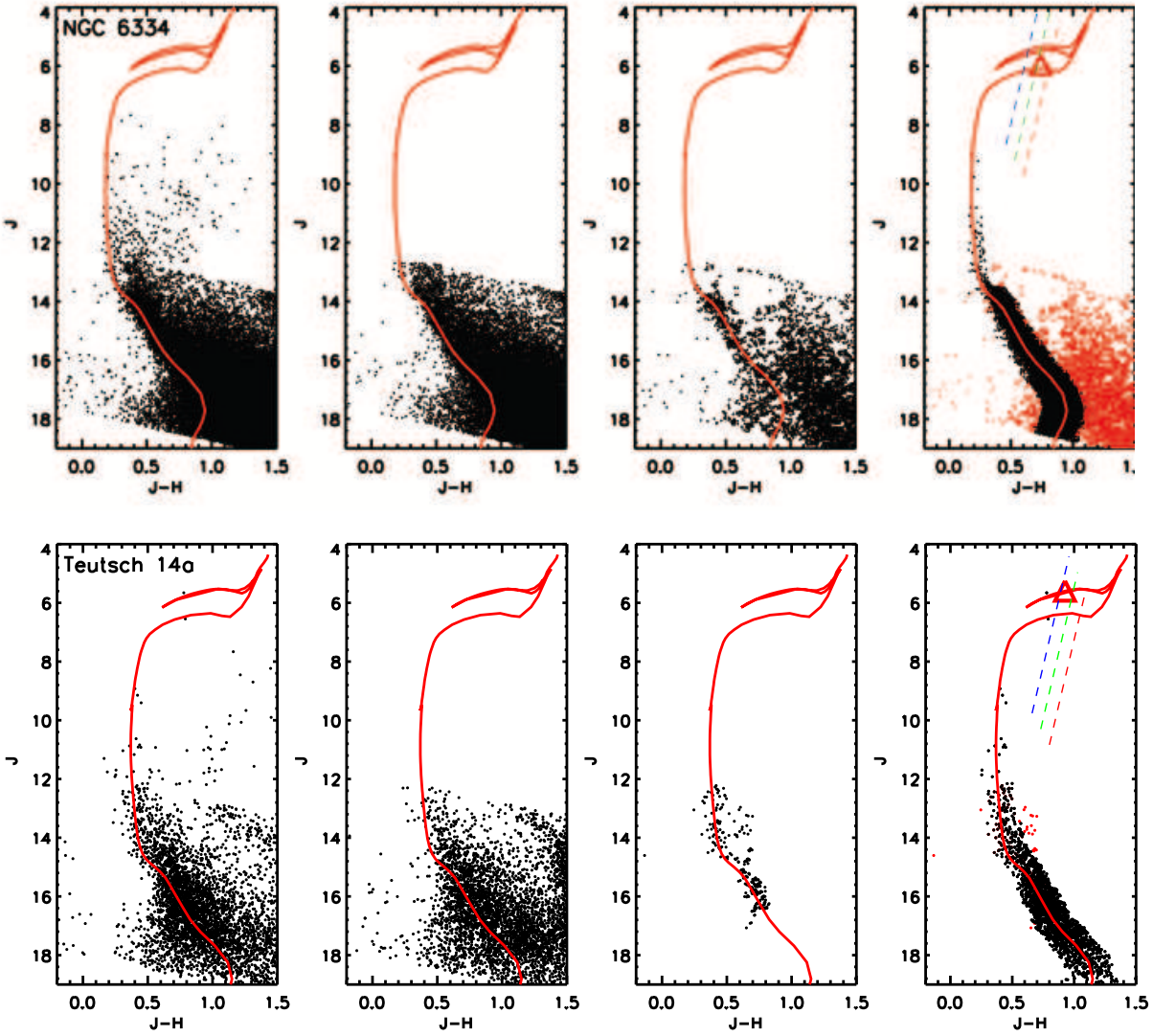

Figure 2. Isochrone fits to the four OC CMDs hosting Cepheids. From left to right: Original CMDs, control-field CMDs, statistically cleaned CMDs and the CMDs resulting from our automated fits. In the original CMDs, the black data points are stars from the combined 2MASS and VVV data sets; in the control-field CMDs, the black data points are stars in the VVV control field. The cleaned CMDs show candidate cluster members, selected by statistically subtracting the control-field CMD from the cluster CMD. The black data points in the CMDs resulting from our automated fits are high-probability OC members; red dots: stars in the cleaned CMDs used to compare with the black dots. Solid red lines: best-fitting isochrones for solar metallicity and different distance moduli, reddening values and ages based on the Padova isochrones (Girardi et al. 2000; Bressan et al. 2012). Green dashed lines: central ridgelines of the Cepheid instability strips converted from Sandage et al. (2008); red and blue dashed lines: red and blue edges of the instability strips, respectively. The Cepheids' JH magnitudes have been converted to mean-intensity magnitudes (see Section 3.3); they are shown as red triangles.

Table 1. Parameters of the four newly discovered VVV OCs. RV: radial velocity.

ID	RA(J2000) (hh:mm:ss)	DEC(J2000) (° ′ ″)	Radius (arcmin)	Distance (kpc)	$E(J-H)$ (mag)	$\log(t)$ [yr]	μ_α (mas yr^{-1})	μ_δ (mas yr^{-1})	RV (km s^{-1})
Teutsch 14a	18:03:31.4	−22:07:31.3	5.0	2.0 ± 0.2	0.48 ± 0.01	7.5 ± 0.3	-0.2 ± 3.9	0.4 ± 4.2	
Majaess 170	16:00:52.0	−51:42:36.6	6.0	1.8 ± 0.2	0.38 ± 0.03	8.1 ± 0.2	-3.2 ± 3.1	-3.1 ± 3.3	
Teutsch 77	11:53:15.6	−62:36:33.2	10.0	2.6 ± 0.3	0.10 ± 0.02	8.1 ± 0.2	-4.2 ± 4.2	-2.0 ± 3.8	
NGC 6334	17:20:52.7	−36:07:02.5	20.0	1.7 ± 0.2	0.28 ± 0.02	7.7 ± 0.3	-1.2 ± 3.1	-0.2 ± 3.4	-4 ± 2

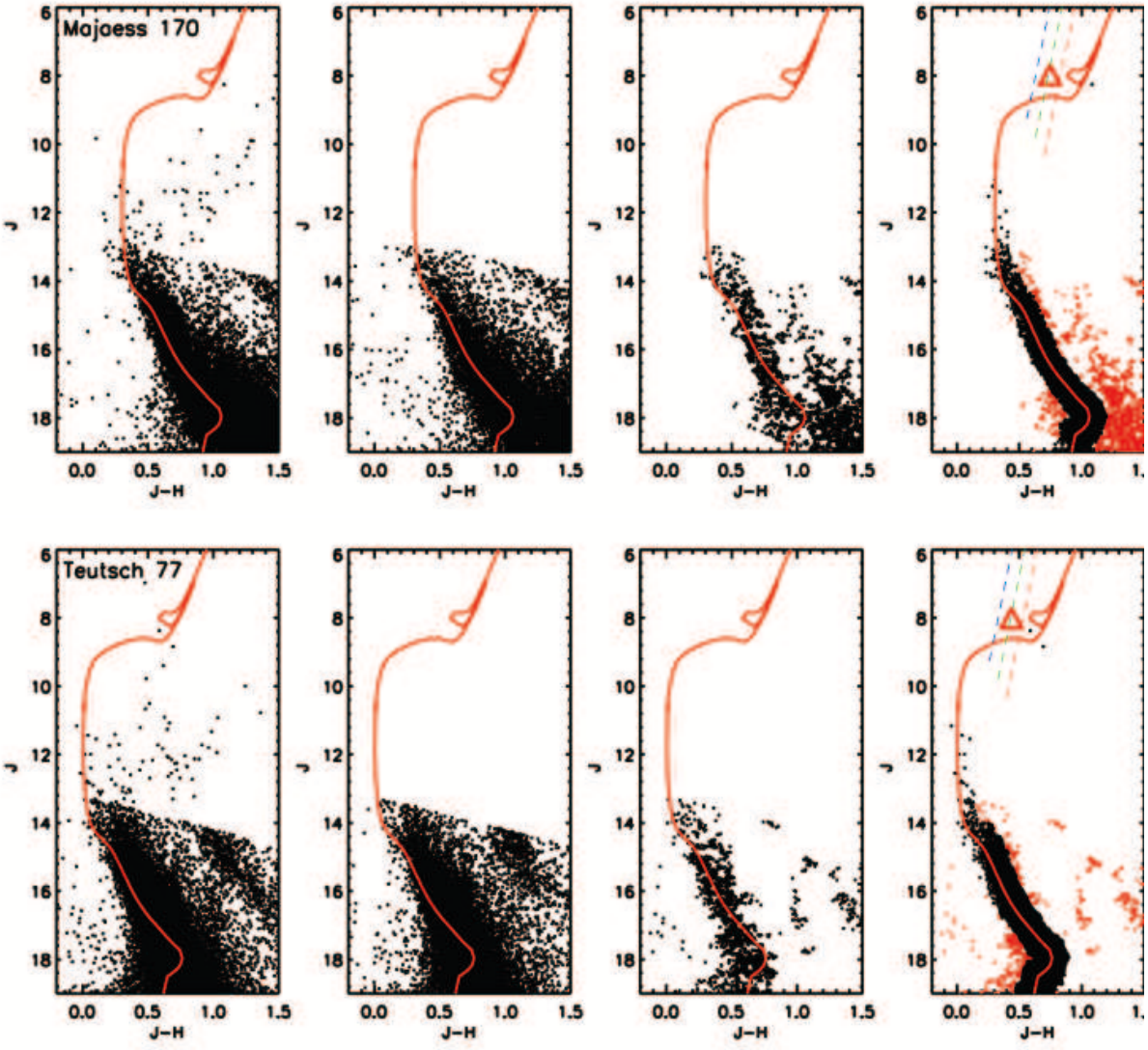

Figure 2. (Continued)

$\log(t\ \mathrm{yr}^{-1}) = (8.31 \pm 0.08) - (0.67 \pm 0.01)\log(P\ \mathrm{day}^{-1})$ for fundamental-mode Cepheids. Therefore, the age of V0470 Sco is $\log(t\ \mathrm{yr}^{-1}) = 7.5 \pm 0.1$. The difference compared with the cluster age is also within the 1σ age error (0.3 dex). Considering all of these constraints, V0470 Sco is a high-confidence OC Cepheid.

Teutsch 14a is a small OC with a size of 7 arcmin (Dias et al. 2002). The Cepheid ASAS J180342−2211.0 is projected onto the cluster centre. Based on the OC's CMD, ASAS J180342−2211.0 is located inside the cluster's instability strip. Teutsch 14a is located in the Galactic bulge and poorly studied. Schultheis et al. (2014) estimated the extinction values of and distances to eight regions inside the 7 arcmin OC radius, resulting in average values of $E(J-H) = 0.51 \pm 0.10$ mag and $d = 2.0 \pm 0.5$ kpc. We determined the cluster's most likely distance, colour excess and age using isochrone fitting, i.e., $\mu_0 = 11.53 \pm 0.23$ mag ($d = 2.0 \pm 0.2$ kpc), $E(J-H) = 0.48 \pm 0.01$ mag and $\log(t\ \mathrm{yr}^{-1}) = 7.5 \pm 0.3$. ASAS J180342−2211.0 has a pulsation period of $\log P = 1.623$ [days]. It is very important in the context of the PLR, since it is one of the longest-period OC Cepheids known in the Galaxy. The Cepheid's age is $\log(t\ \mathrm{yr}^{-1}) = 7.2 \pm 0.1$, which is within the range inferred for the cluster's age. The proper motion of Teutsch 14a is $(\mu_{\alpha,\mathrm{cl}}, \mu_{\delta,\mathrm{cl}}) = (-0.2 \pm 3.9, 0.4 \pm 4.2)$ mas yr^{-1}, which is comparable to the values determined by Dias et al. (2014). The Cepheid's proper motion is $(\mu_{\alpha,\mathrm{Cep}}, \mu_{\delta,\mathrm{Cep}}) = (-0.6 \pm 3.3, 5.9 \pm 2.5)$ mas yr^{-1}, just inside the 1σ boundary of cluster's proper-motion distribution. Although radial-velocity data are not available, ASAS J180342−2211.0 has all attributes to make it a high-confidence OC Cepheid.

Majaess 170 is a small OC with a size of 5 arcmin (Dias et al. 2002). ASAS J160125−5150.3 is located 7 arcmin from the cluster centre. This cluster has not been studied previously. The distance modulus, colour excess and age we determined are $\mu_0 = 11.30 \pm 0.28$ mag ($d = 1.8 \pm 0.3$ kpc), $E(J-H) = 0.38 \pm 0.03$ mag and $\log(t\ \mathrm{yr}^{-1}) = 8.1 \pm 0.2$, respectively. The proper motions of this OC–Cepheid pair are $(\mu_{\alpha,\mathrm{cl}}, \mu_{\delta,\mathrm{cl}} = (-3.2 \pm 3.1, -3.1 \pm 3.3)$ mas yr^{-1} and $(\mu_{\alpha,\mathrm{Cep}}, \mu_{\delta,\mathrm{Cep}}) = (-1.3 \pm 1.8, -0.2 \pm 1.8)$ mas yr^{-1}. The

Cepheid's proper-motion and distance-modulus measurements imply that it is a high-probability cluster member. The age of ASAS J160125−5150.3, derived from its period, is approximately $\log(t\ \mathrm{yr}^{-1}) = 7.8 \pm 0.1$, which implies a difference with respect to the host cluster of less than 0.3 dex.

Finally, Teutsch 77 is a small OC with a size of 7 arcmin (Dias et al. 2002). BB Cen is located 15 arcmin from the cluster centre. The Cepheid's proper motion, $(\mu_{\alpha,\mathrm{Cep}}, \mu_{\delta,\mathrm{Cep}}) = (-3.9 \pm 1.3, 1.0 \pm 1.1)$ mas yr^{-1}, is within the 1σ range of the cluster's average proper motion, $(\mu_{\alpha,\mathrm{cl}}, \mu_{\delta,\mathrm{cl}}) = (-4.2 \pm 4.2, -2.0 \pm 3.8)$ mas yr^{-1}. We obtained $\mu_0 = 12.40 \pm 0.25$ mag ($d = 2.6 \pm 0.3$ kpc), $E(J-H) = 0.10 \pm 0.02$ mag and $\log(t\ \mathrm{yr}^{-1}) = 8.1 \pm 0.2$. A comparison of the cluster and Cepheid properties suggests that BB Cen is an OC Cepheid.

4 NEAR-INFRARED PERIOD–LUMINOSITY RELATIONS

In attempting to establish Cepheid NIR PLRs, we run into the problem that only some Cepheids have complete NIR light curves. Monson & Pierce (2011) published JHK photometry for 131 northern Galactic classical Cepheids, while JHK mean magnitudes in the South African Astronomical Observatory (SAAO) system are available for 223 southern Cepheids (van Leeuwen et al. 2007). The mean NIR magnitudes have been measured directly for only 19 OC Cepheids (Chen et al. 2015). To supplement these data sets with OC Cepheids without readily available NIR light curves, we need to transform single-epoch NIR magnitudes to mean magnitudes. Fortunately, Cepheid NIR light curves are related to their V-band light curves, so that we can estimate the mean NIR magnitudes based on the corresponding V-band light curves (Soszyński et al. 2005). The amplitudes of Cepheid light curves decrease from the optical to the NIR regime. The NIR-to-optical amplitude ratio is around 0.3–0.4. These considerations allow us to derive the OC Cepheids' NIR amplitudes. We calculated the phases of the single-epoch NIR magnitudes and combined them with the seven Fourier coefficients of the light-curve template from Soszyński et al. (2005). This light-curve template was developed based on 30 Cepheids in the Galaxy and 31 Cepheids in the Large Magellanic Cloud (LMC) with complete $VIJHK_\mathrm{s}$ light curves. The JHK_s light-curve template was developed with respect to the V-band light curve. The resulting differences between the derived and real mean magnitudes are less than 0.03 mag, which is acceptable because this level of uncertainty is small compared with the uncertainty in the distance modulus. We thus obtained JHK_s mean magnitudes from 2MASS single-epoch photometry for seven additional Cepheids without directly measured NIR mean magnitudes, including AP Vel, CG Cas, V0367 Sct, V0470 Sco, ASASJ182714−1507.1, ASAS J180342−2211.0 and ASAS J160125−5150.3 (see Table 3).

Establishing and calibrating PLRs is vital for the use of Cepheids as distance tracers, especially when using multiple passbands in the NIR. The use of OCs to derive PLRs is a useful and independent method. Tammann et al. (2003) derived BVI PLRs for 25 OC Cepheids, An et al. (2007) obtained $BVI_\mathrm{c}JHK_\mathrm{s}$ PLRs based on seven well-studied OC Cepheids and Chen et al. (2015) obtain a J-band PLR based on 19 OC Cepheids. In this paper, we determined the JHK_s PLRs based on 31 OC Cepheids. This represents a significant improvement in the J-band PLR of Chen et al. (2015), while statistically meaningful H- and K_s-band OC–Cepheid PLRs were determined for the first time:

$$\begin{aligned}
&\langle M_J\rangle = (-3.077 \pm 0.090)[\log P - 1] - (5.279 \pm 0.028), \sigma_J = 0.148;\\
&\langle M_H\rangle = (-3.167 \pm 0.075)[\log P - 1] - (5.601 \pm 0.023), \sigma_H = 0.124;\\
&\langle M_{K\mathrm{s}}\rangle = (-3.224 \pm 0.073)[\log P - 1] - (5.693 \pm 0.022), \sigma_{K\mathrm{s}} = 0.120.
\end{aligned} \quad (1)$$

These are currently the most accurate PLRs based on the largest OC Cepheid sample available to date, characterized by an accuracy that is improved by 40 per cent compared with previous determinations. The PLRs derived here agree well with results based on other methods (An et al. 2007; Ngeow 2012), considering the uncertainties: see Fig. 3. The J-band PLRs exhibit obvious zero-point differences. These zero-point differences become smaller from J to K_s, and in the K_s band the differences among the three relations are always less than 0.06 mag. In addition, for the J-band PLRs, we find at the short-period end – $\log P \simeq 0.4$ [days] – a 0.14 mag difference between An et al. (2007) and Ngeow (2012), while our PLR yields a compromise value. At the long-period end – $\log P \simeq 1.6$ [days] – these differences disappear. This is owing to the small number of long-period (high-mass) Cepheids, which play an important role in constraining the slope of the PLR. The slopes we have determined here are comparable with those of Ngeow (2012). With respect to the slopes determined by An et al. (2007), however, we find differences of 0.08, 0.06 and 0.06 mag in the J, H and K_s bands, respectively. Since our PLR slopes and those of Ngeow (2012) were derived based on Galactic Cepheids, while the slopes of An et al. (2007) used the PLR slopes of Cepheids in the LMC as their basis, this suggests that the PLR slopes may be different for the LMC and the Galaxy, even at NIR wavelengths. However, these differences may also have been caused by the application of different methods by their respective authors. The slopes and intercepts of the three sets of JHK_s PLRs are listed in Table 4. In view of the prevailing uncertainties, we cannot firmly conclude that the differences cited above are statistically significant. Additional Cepheid samples are needed to constrain the statistical uncertainties.

5 CONCLUSION

The availability of VVV DR1 provides a unique opportunity to uncover and study faint and highly obscured OCs in the Galactic plane near the Galactic Centre. Using the DAML02 OC catalogue and other new OCs found in the VVV data, we have carefully examined 22 OCs and discovered four new OC Cepheids. Parameters such as distances, reddening values and ages were better determined compared with previous work based on isochrone fitting. By comparison of distances, apparent positions, proper motions and ages of the clusters and Cepheids, the newly found OC–Cepheid pairs include NGC 6334 and V0470 Sco, Teutsch 14a and ASAS J180342−2211.0, Majaess 170 and ASAS J160125−5150.3, and Teutsch 77 and BB Cen. ASAS J180342−2211.0 is the longest-period Cepheid – $\log P = 1.623$ [days] – thus far

Table 2. Properties of our sample of 31 OCs and Cepheids.

Cluster	$E(J-H)$ (mag)	$\log(P)$ [day]	$\log(t)$ [yr]	μ_0 (mag)	Cepheid	$\langle J\rangle$ (mag)	$\langle H\rangle$ (mag)	$\langle K_{\rm s}\rangle$ (mag)	M_J (mag)	M_H (mag)	$M_{K{\rm s}}$ (mag)
Dolidze 34	0.36 ± 0.02	1.043	7.9 ± 0.2	11.85 ± 0.25	TY Sct	7.23(0.01)	6.62(0.01)	6.40(0.01)	−5.57(0.27)	−5.82(0.25)	−5.83(0.23)
Dolidze 34	0.36 ± 0.02	1.000	7.9 ± 0.2	11.85 ± 0.25	CN Sct	7.82(0.01)	7.06(0.01)	6.73(0.01)	−4.98(0.27)	−5.38(0.25)	−5.50(0.23)
Ruprecht 65	0.2 ± 0.03	0.495	8.0 ± 0.2	11.07 ± 0.38	AP Vel	7.81(0.05)	7.36(0.09)	7.18(0.05)	−3.79(0.43)	−4.04(0.44)	−4.10(0.38)
Dolidze 52	0.24 ± 0.02	0.808	7.6 ± 0.3	10.77 ± 0.25	XX Sgr	6.44(0.02)	5.98(0.02)	5.82(0.02)	−4.96(0.27)	−5.18(0.25)	−5.20(0.24)
NGC 6683	0.18 ± 0.01	0.870	8.2 ± 0.2	11.62 ± 0.23	CK Sct	7.38(0.01)	6.81(0.01)	6.63(0.01)	−4.72(0.24)	−5.11(0.23)	−5.19(0.22)
Berkeley 58	0.23 ± 0.02	0.640	8.0 ± 0.2	12.39 ± 0.35	CG Cas	8.95(0.09)	8.44(0.05)	8.26(0.03)	−4.05(0.44)	−4.33(0.38)	−4.38(0.36)
NGC 7790	0.14 ± 0.02	0.688	7.9 ± 0.2	12.63 ± 0.35	CF Cas	8.60(0.01)	8.11(0.01)	7.94(0.01)	−4.41(0.37)	−4.75(0.35)	−4.84(0.33)
NGC 6087	0.06 ± 0.005	0.989	8.0 ± 0.2	9.84 ± 0.11	S Nor	4.68(0.02)	4.30(0.02)	4.15(0.02)	−5.32(0.13)	−5.64(0.13)	−5.76(0.13)
IC 4725	0.18 ± 0.01	0.829	7.8 ± 0.2	8.82 ± 0.13	U Sgr	4.52(0.01)	4.09(0.01)	3.95(0.01)	−4.78(0.14)	−5.03(0.13)	−5.06(0.12)
vdBergh 1	0.26 ± 0.015	0.731	7.9 ± 0.2	11.11 ± 0.24	CV Mon	7.31(0.01)	6.77(0.01)	6.57(0.01)	−4.49(0.25)	−4.77(0.24)	−4.82(0.23)
NGC 129	0.165 ± 0.015	0.903	7.8 ± 0.2	11.16 ± 0.24	DL Cas	6.56(0.01)	6.09(0.01)	5.93(0.01)	−5.04(0.25)	−5.35(0.24)	−5.41(0.23)
Collinder 394	0.095 ± 0.005	0.822	8.0 ± 0.2	9.35 ± 0.16	BB Sgr	5.05(0.02)	4.66(0.02)	4.50(0.02)	−4.55(0.18)	−4.84(0.18)	−4.95(0.18)
Turner 2	0.18 ± 0.01	1.339	8.0 ± 0.2	11.22 ± 0.13	WZ Sgr	5.26(0.01)	4.74(0.01)	4.57(0.01)	−6.44(0.14)	−6.78(0.13)	−6.84(0.12)
Teutsch 14a	0.48 ± 0.01	1.623	7.5 ± 0.3	11.53 ± 0.23	180342−2211.0	5.59(0.07)	4.76(0.07)	4.28(0.06)	−7.21(0.29)	−7.56(0.29)	−7.76(0.27)
Majaess 170	0.38 ± 0.03	0.699	8.1 ± 0.2	11.30 ± 0.28	160125−5150.3	7.97(0.02)	7.22(0.04)	6.90(0.03)	−4.33(0.30)	−4.70(0.29)	−4.79(0.26)
Lynga 6	0.38 ± 0.02	1.033	7.9 ± 0.2	11.66 ± 0.25	TW Nor	7.45(0.02)	6.72(0.02)	6.39(0.02)	−5.25(0.27)	−5.58(0.25)	−5.68(0.24)
Teutsch 77	0.1 ± 0.02	0.757	8.1 ± 0.2	12.04 ± 0.25	BB Cen	8.00(0.02)	7.57(0.02)	7.39(0.02)	−4.30(0.27)	−4.63(0.25)	−4.76(0.24)
NGC 6334	0.28 ± 0.02	1.211	7.7 ± 0.3	11.16 ± 0.25	V0470 Sco	5.95(0.07)	5.21(0.07)	4.87(0.06)	−5.95(0.32)	−6.41(0.30)	−6.59(0.28)
Kharchenko 3	0.26 ± 0.025	0.744	8.1 ± 0.2	11.51 ± 0.37	182714−1507.1	7.89(0.05)	7.32(0.04)	7.14(0.04)	−4.31(0.42)	−4.62(0.38)	−4.65(0.36)
ASCC 61	0.08 ± 0.01	0.687	8.0 ± 0.2	11.19 ± 0.23	SX Car	7.26(0.02)	6.88(0.02)	6.74(0.02)	−4.14(0.25)	−4.44(0.24)	−4.53(0.23)
ASCC 61	0.08 ± 0.01	1.277	8.0 ± 0.2	11.19 ± 0.23	VY Car	5.41(0.02)	4.97(0.02)	4.79(0.02)	−5.99(0.25)	−6.35(0.24)	−6.48(0.23)
ASCC 69	0.06 ± 0.01	0.985	8.0 ± 0.2	9.74 ± 0.23	S Mus	4.50(0.02)	4.15(0.02)	4.00(0.02)	−5.40(0.25)	−5.69(0.24)	−5.80(0.23)
Collinder 220	0.12 ± 0.015	0.728	8.1 ± 0.2	11.48 ± 0.24	UW Car	7.31(0.02)	6.92(0.02)	6.67(0.02)	−4.49(0.26)	−4.76(0.24)	−4.94(0.24)
Feinstein 1	0.12 ± 0.01	1.589	7.0 ± 0.3	10.88 ± 0.23	U Car	4.14(0.02)	3.69(0.02)	3.51(0.02)	−7.06(0.25)	−7.39(0.24)	−7.50(0.23)
Trumpler 35	0.33 ± 0.01	1.294	7.8 ± 0.2	11.43 ± 0.18	RU Sct	5.89(0.01)	5.27(0.01)	5.07(0.01)	−6.41(0.19)	−6.70(0.18)	−6.71(0.17)
Ruprecht 175	0.065 ± 0.01	1.215	7.8 ± 0.2	10.23 ± 0.18	X Cyg	4.42(0.02)	3.98(0.02)	3.82(0.02)	−5.98(0.20)	−6.36(0.19)	−6.48(0.18)
NGC 5662	0.1 ± 0.01	0.740	8.0 ± 0.2	9.24 ± 0.13	V Cen	5.02(0.02)	4.65(0.02)	4.49(0.02)	−4.48(0.15)	−4.75(0.14)	−4.85(0.13)
Alessi 95	0.08 ± 0.02	0.440	8.0 ± 0.2	8.04 ± 0.20	SU Cas	4.49(0.02)	4.22(0.02)	4.11(0.02)	−3.77(0.22)	−3.95(0.20)	−4.01(0.19)
NGC 1647	0.1 ± 0.01	0.651	8.2 ± 0.2	8.74 ± 0.13	SZ Tau	4.78(0.02)	4.43(0.02)	4.30(0.02)	−4.22(0.15)	−4.47(0.14)	−4.54(0.13)
NGC 6649	0.42 ± 0.01	0.651	8.1 ± 0.2	10.89 ± 0.13	V0367 Sct	7.66(0.03)	6.98(0.04)	6.67(0.04)	−4.34(0.16)	−4.60(0.16)	−4.66(0.15)
NGC 6067	0.12 ± 0.02	1.053	8.0 ± 0.2	11.22 ± 0.25	V0340 Nor	6.26(0.01)	5.73(0.01)	5.60(0.01)	−5.29(0.27)	−5.68(0.25)	−5.79(0.23)

Table 3. Mean magnitudes of seven Cepheids. $J(\varphi)$, $H(\varphi)$ and $K_{\rm s}(\varphi)$ are 2MASS magnitudes at phase φ, while $\langle J\rangle$, $\langle H\rangle$ and $\langle K_{\rm s}\rangle$ are the derived mean magnitudes.

Cepheid	Amp(V) (mag)	Phase (φ)	$J(\varphi)$ (mag)	$H(\varphi)$ (mag)	$K_{\rm s}(\varphi)$ (mag)	$\langle J\rangle$ (mag)	$\langle H\rangle$ (mag)	$\langle K_{\rm s}\rangle$ (mag)
V0367 Sct	0.54	0.42	7.716(0.024)	7.004(0.027)	6.681(0.021)	7.657(0.034)	6.983(0.043)	6.671(0.038)
CG CAS	0.27	0.84	8.832(0.044)	8.313(0.033)	8.136(0.021)	8.954(0.086)	8.435(0.050)	8.257(0.034)
AP Vel	0.00	0.72	7.730(0.026)	7.351(0.059)	7.188(0.017)	7.807(0.052)	7.355(0.090)	7.181(0.048)
180342−2211.0	0.84	0.76	5.658(0.021)	4.880(0.042)	4.403(0.033)	5.590(0.065)	4.764(0.069)	4.277(0.057)
160125−5150.3	0.06	0.30	7.921(0.018)	7.205(0.026)	6.889(0.020)	7.968(0.023)	7.223(0.036)	6.902(0.031)
V0470 Sco	0.95	0.92	5.900(0.027)	5.245(0.024)	4.919(0.023)	5.949(0.072)	5.209(0.066)	4.869(0.064)
182714−1507.1	0.79	0.64	7.977(0.020)	7.415(0.020)	7.227(0.024)	7.894(0.054)	7.324(0.036)	7.136(0.037)

found in an OC, which is important in the context of constraining the slope of the PLR.

The currently most complete NIR Cepheid PLRs based on 31 OC Cepheids were obtained (a significant improvement from the previous PLRs which were based on up to 19 OC Cepheids), i.e., $\langle M_J\rangle = (-3.077\pm0.090)\log P-(2.202\pm0.090)$, $\langle M_H\rangle = (-3.167\pm0.075)\log P-(2.434\pm0.074)$ and $\langle M_{Ks}\rangle = (-3.224\pm0.073)\log P-(2.469\pm0.072)$. The associated uncertainties have been improved by 40 per cent compared with previous Cepheid PLRs based on the OC-matching method. Our PLRs are in good agreement with the best NIR PLRs available for all Galactic Cepheids obtained using other methods. Particularly in the $K_{\rm s}$ band, the zero-point differences are very small; differences of less than 0.06 mag are expected for any Cepheid.

Since there are more than 20,000 Cepheids and 20,000 OCs in the Galaxy, we expect that thousands of OC Cepheids will be discovered in the future. *Gaia* will observe some 9000 Cepheids (Windmark et al. 2011), which will improve the distances, proper motions and radial velocities of not only the Cepheids but also their host clusters. By combining the more accurate parallax distances from *Gaia* with OC distances based on isochrone fitting, the Cepheid PLRs will be left with only small systematic errors.

We thank the referees for their comments. We are grateful for support from the National Natural Science Foundation of China through grants 11633005, U1631102, 11373010 and 11473037.

REFERENCES

An D., Terndrup D. M., Pinsonneault M. H., 2007, ApJ, 671, 1640

Anderson L. D., Bania T. M., Balser D. S., et al. 2011, ApJS, 194, 32

Anderson R. I., Eyer L., Mowlavi N. 2013, MNRAS, 434, 2238

Benedict G. F., et al., 2007, AJ, 133, 1810

Bono G., Marconi M., Cassisi S., Caputo F., Gieren W. P., Pietrzyński G., 2005, ApJ, 621, 966

Borissova J., Bonatto C., Kurtev R. et al., 2011, A&A, 532, 131

Borissova J., Chené, A. N. et al., 2014, A&A 569, 24

Bressan A., Marigo P., Girardi L. et al., 2012, MNRAS, 427, 127

Chen X. D., de Grijs R., Deng L. C., 2015, MNRAS, 446, 1268

Chené, A.-N, Borissova, J., Clarke, J. R. A. et al., 2012, A&A, 545, 54

Table 4. Slopes (a) and intercepts (b) of the NIR PLRs derived by An et al. (2007), Ngeow (2012) and in this paper. The PLRs are defined as $\langle M\rangle = a[\log P - 1] + b$, where M are the intrinsic magnitudes and P the Cepheids' periods.

	$a(J)$	$b(J)$	$a(H)$	$b(H)$	$a(K_{\rm s})$	$b(K_{\rm s})$
An07	-3.148 ± 0.053	-5.271 ± 0.076	-3.233 ± 0.044	-5.593 ± 0.069	-3.282 ± 0.040	-5.718 ± 0.064
Ngeow12	-3.058 ± 0.021	-5.340 ± 0.019	-3.181 ± 0.022	-5.648 ± 0.020	-3.231 ± 0.021	-5.732 ± 0.020
This paper	-3.077 ± 0.090	-5.279 ± 0.028	-3.167 ± 0.075	-5.601 ± 0.023	-3.224 ± 0.073	-5.693 ± 0.022

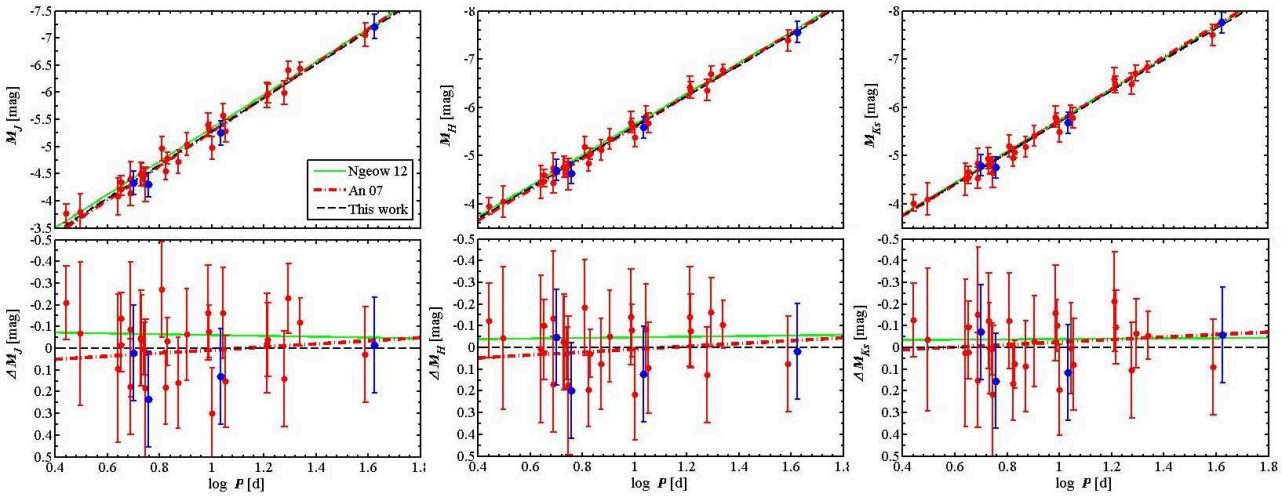

Figure 3. (Top) $JHK_{\rm s}$ PLRs for 31 OC Cepheids. Red bullets: confirmed OC Cepheids; blue bullets: new, high-confidence OC Cepheids found in this paper. The green solid line is the $JHK_{\rm s}$ PLR for Galactic Cepheids (Ngeow 2012); the red dotted line is from An et al. (2007) and the black dashed line is our linear fit. (Bottom) Differences between the three PLRs, where our newly determined PLR is used as reference.

Cutri R. M., et al., 2003, The 2MASS Catalogue of Point Sources, Univ. Massachusetts & IPAC/CalTech

Dambis A. K., Berdnikov L. N. et al., 2015, AstL, 41, 489

Dékány I., Minniti D., Hajdu G. et al., 2015, ApJ, 799, L11

Dias W. S., Alessi B. S., Moitinho A., Lépine J. R. D., 2002, A&A 389, 871

Dias W. S., Monteiro, H. et al., 2014, A&A, 564, 79

Feast M. W., Catchpole R. M., 1997, MNRAS, 286, L1

Feast M. W., Menzies J. W., Matsunaga N., Whitelock P. A., 2014, Nature, 509, 342

Freedman W. L., Madore B. F., Scowcroft V. et al., 2011, AJ, 142, 192

Gieren W. P., Fouqué P., Gomez M. I., 1997, ApJ, 488, 74

Girardi, L., Bressan, A., Bertelli, G., Chiosi, C. 2000, A&AS, 141, 371

Kharchenko N. V., Piskunov A. E., Schilbach E., Röser S., Scholz R.-D., 2013, A&A 558, 53

Leavitt, H. S., Pickering, E. C. 1912, Harvard College Observatory Circular, 173, 1

Lucas P. W., Hoare M. G., Longmore A., Schroeder A. C., et al., 2008, MNRAS, 391, 136

Majaess D. J., Turner D. G., Lane D. J., 2009, JAVSO, 37, 179

Majaess D., et al., 2011, ApJ, 741, L27

Majaess D., Turner D. G., Gallo L., Gieren W., Bonatto C., Lane D. J., Balam D., Berdnikov L., 2012, ApJ, 753, 144

Majaess D., Turner D. G. et al., 2012, A&A, 537, L4

Majaess D., Carraro G., Moni Bidin C. et al., 2013, A&A, 560, 22

Matsunaga N., Kawadu T., Nishiyama S. et al., 2011, Nature, 477, 188

Matsunaga N., Fukue K., Yamamoto R. et al., 2015, ApJ, 799, 46

Minniti, D. et al., 2010, New Astronomy, 15, 433

Monson A. J., Pierce M. J., 2011, ApJS, 193, 12

Ngeow C. C., 2012, ApJ, 747, 50

Pejcha O., & Kochanek C. S., 2012, ApJ, 748, 107

Riess A. G., Macri L., Casertano S. et al., 2011, ApJ, 730, 119

Russeil D., Zavagno A., Adami C. et al., 2012, A&A, 538, 142

Russeil D., Schneider N., Anderson L. et al., 2013, A&A, 554, 42

Saito R. K., Hempel M., Minniti D. et al., 2012, A&A, 537, 107

Sandage A., Tammann G. A., 2008, ApJ, 686, 779

Schmeja S., Kharchenko N. V., Piskunov A. E. et al., 2014, A&A 568, 51

Scholz R. D., Kharchenko N. V., Piskunov A. E. et al., 2015, A&A 581, 39

Schultheis M., Zasowski G., Allende Prieto, C. et al., 2014, AJ, 148, 24

Soszyński I., Gieren W., Pietrzyński G., 2005, PASP, 117, 823

Storm J., et al., 2011, A&A, 534, A94

Pojmanski G. 2002, AcA, 52, 397
Tammann G. A., Sandage A., Reindl B., 2003, A&A, 404, 423
Turner D. G., 2010, Ap&SS, 326, 219
Turner D. G., Majaess D. J., Lane, D. J. et al., 2012, MNRAS, 422, 2501
van Leeuwen, F., Feast, M.W., Whitelock, P. A., Laney, C. D., 2007, MNRAS, 379, 723
Windmark F., Lindegren L., Hobbs D., 2011, A&A, 530, 76
Zacharias N., Finch C. T., Girard T. M. et al., 2013, AJ, 145, 44